Journal of Sound and Vibration 338 (2015) 42–59

Contents lists available at ScienceDirect

Journal of Sound and Vibration

journal homepage: www.elsevier.com/locate/jsvi

Natural frequencies, modeshapes and modal interactions for strings vibrating against an obstacle: Relevance to Sitar and Veena

A.K. Mandal *, P. Wahi

Indian Institute of Technology Kanpur, Kanpur, Uttar Pradesh 208016, India

ARTICLE INFO

Article history:
Accepted 7 June 2014
Handling Editor: A.V. Metrikine

ABSTRACT

We study the vibration characteristics of a string with a smooth unilateral obstacle placed at one of the ends similar to the strings in musical instruments like sitar and veena. In particular, we explore the correlation between the string vibrations and some unique sound characteristics of these instruments like less inharmonicity in the frequencies, a large number of overtones and the presence of both frequency and amplitude modulations. At the obstacle, we have a moving boundary due to the wrapping of the string and an appropriate scaling of the spatial variable leads to a fixed boundary at the cost of introducing nonlinearity in the governing equation. Reduced order system of equations has been obtained by assuming a functional form for the string displacement which satisfies all the boundary conditions and gives the free length of the string in terms of the modal coordinates. To study the natural frequencies and mode-shapes, the nonlinear governing equation is linearized about the static configuration. The natural frequencies have been found to be harmonic and they depend on the shape of the obstacle through the effective free length of the string. Expressions have been obtained for the time-varying mode-shapes as well as the variation of the nodal points. Modal interactions due to coupling have been studied which show the appearance of higher overtones as well as amplitude modulations in our theoretical model akin to the experimental observations. All the obtained results have been verified with an alternate formulation based on the assumed mode method with polynomial shape functions.

© 2014 Elsevier Ltd. All rights reserved.

1. Introduction

Sitar, veena, tanpura (also known as tambura) etc. are some Indian stringed musical instruments [1] which have a common constructional feature that they have a finite-sized curved bridge at one end instead of a sharp bridge which is commonly used in western stringed instruments [2]. In these instruments the string wraps and unwraps around the curved bridge while vibrating. . Thereby, the string keeps changing its effective length which makes it a moving boundary problem for the string vibrating against a one sided obstacle. These musical instruments have an attractive tonal quality in terms of harmonicity, modulation in frequency and amplitude. Our aim in this paper is to understand the relation between the presence of the finite bridge and these unique sound characteristics.

* Corresponding author at: Department of Mechanical Engineering, Indian Institute of Technology Kanpur, Kanpur, India.
E-mail address: ashok.mndl@gmail.com (A.K. Mandal).

http://dx.doi.org/10.1016/j.jsv.2014.06.010
0022-460X/© 2014 Elsevier Ltd. All rights reserved.

Nomenclature

b	nondimensional length of the bridge
B	length of the bridge along the X-direction
h_r	nondimensional height of the string at the right end
T	tension in the string
x	scaled position of string element in the X-direction
$\overline{x}$	nondimensional position of a string element in the X-direction
y_{st}	transverse displacement of the string for the static configuration
$\overline{y}(=y)$	nondimensional transverse displacement of the string
$\tilde{y}$	small displacement of the string about its static configuration
Y	transverse displacement of the string
Y_B	geometry of the bridge
α	curvature of the bridge
β_n	modal coordinates
γ	nondimensional contact length of the string on the bridge
γ_{st}	contact length of the string on the bridge for the static configuration
$\tilde{\gamma}$	small perturbation in the contact length
Γ	contact length of the string on the bridge along X-direction
ρ	density of the string per unit length
$\overline{\tau}(=\tau)$	nondimensional time

Several experimental studies on the acoustics of the Indian stringed musical instruments especially the sitar and the tanpura have been reported in the literature [2–11]. In the early twentieth century, Raman [2] noted that all string frequencies in these instruments are excited irrespective of the location of the excitation thereby violating the Young–Helmholtz law which states that the vibrations of a string do not contain the natural modes which have a node at the point of excitation. He notes that this is because of the special form of the bridge but did not explain the reason behind the inapplicability of the Young–Helmholtz law. It has been understood now that the nodal points of the different modes for the string vibrations are not stationary due to the finite bridge and hence, all modes will be excited irrespective of the location of the excitation. Janakiram and Yegnarayan [3] found that the tonal spectrum of tanpura sound is not stationary but is time varying. A follow-up investigation by Houtsma and Burns [4] determined that upto 30 partials of the fundamental frequency are nearly harmonic for the tanpura. Benade and Messenger [5] have reported that the sitar tone has complex time behavior but well-marked pitch along with the presence of modulation in frequency and amplitude of the various modes. In a related study, Sengupta et al. [6] have observed the presence of vibratos (or frequency modulation) of different character associated with different modes and amplitude modulation for the fundamental frequency in the tanpura sound. Conte et al. performed acoustical measurements on vina (or veena) and tried to extract the mechanical properties of the string as well as the structure from the resonant frequencies. Singh [8] studied the interaction between the frequency characteristics of different strings supported on the same bridge in a sitar and the resulting acoustic patterns. Sitar also has 'sympathetic strings' which are never excited directly but they vibrate due to the vibration of the top plate which itself gets its vibrations from the main strings. The role of these strings in determining the acoustical characteristics of sitar has been discussed by Bahn [9] and Weisser and Demoucron [10]. In all the above cases, the strings vibrate against a smooth obstacle (the bridge).

The bridge used in tanpura and sitar is the same by construction. However, tanpura has an additional feature which is the presence of the juari (a cotton thread placed between the string and the bridge). The sound characteristics of tanpura is significantly modified by the presence of the juari which effectively introduces a non-smoothness in the bridge geometry leading to a sudden change in the free length in contrast to the sitar where the effective length changes smoothly. Raman [2] noted that the non-smooth contact with the bridge facilitates greater amount of energy communication through impulses which add powerful sequence of overtones which were initially absent. Another study done by Carterette et al. [11] showed that the pitch of a tanpura sound without juari was very close to the fundamental and the partials were nearly linear in decibels. The pitch of the tanpura sound with juari was heard one or even two octaves above the base pitch. Also, they reported that the partials upto 20 were significantly powerful. Valette et al. [12] also emphasized the importance of impacts in the generation of higher overtones for the tanpura. A similar kind of mechanism is also found in some Japanese stringed musical instruments like biwa and shamisen where a narrow groove is made on the bridge to introduce non-smoothness. A study done by Taguti and Tohnai [13] shows that this mechanism helps to intensify the higher overtones and elongate the amplitude decay time. In this paper, we show that the higher overtones are generated even in the absence of any impact because of modal interactions introduced by the presence of the curved bridge. However, the energy content in the higher overtones may not match the ones where impact is predominant.

On the theoretical front, Amerio [14] mathematically formulated the problem of vibration of a string against a rigid wall with the assumption that the impact between the wall and string is elastic and provided conditions for admissible solutions. Schatzman [15] extended the analysis of Amerio and showed that uniqueness of solutions requires an extra energy condition to be imposed. Burridge et al. [16] addressed the string vibration problem considering inelastic impact of the string with a rigid parabolic bridge and discussed the nature of the solutions as well as the motion of the free boundary point. Ahn [17] investigated the problem further and found that energy is conserved even with an elastic impact only for special shapes of the obstacle. Taguti [18] modeled deformations in the cross-section of the string during contact while studying the vibrations of string for a Japanese musical instrument called biwa, where he found that the forces responsible

for the elastic deformation of the string during impact result in a gradual build up of high frequency oscillations. Vyasarayani et al. [19] followed Burridge et al. [16] but added an extra condition of smooth wrapping and unwrapping of the string around the bridge which leads to the study of steady-state solutions. They also studied string motions which involve transition from wrapping–unwrapping to fully wrapped or unwrapped which is not very relevant to the string vibrations in musical instruments. Alsahlani and Mukherjee [20] considered perfectly inelastic collision for the string on the obstacle and conclude that the obstacle acts like a damping mechanism to dissipate energy. In all these studies, the string does not approach the obstacle with impending zero velocity and hence, impacts leading to non-conservation of energy are observed. The presence of higher overtones has mostly been attributed to this phenomenon. In contrast, we have considered the case where the string approaches the obstacle with zero velocity but still we observe that higher overtones appear as a result of the nonlinearity associated with the wrapping and unwrapping over the obstacle.

Almost all theoretical studies on vibrations of strings in stringed musical instruments assume planar motion but in reality these strings exhibit a dominant non-planar motion due to the excitation mechanism as well as the presence of the obstacle. The analysis of non-planar motion of strings over curved obstacle is quite complicated and it has not been considered in the present paper as well. However, we point out that there are several studies on the nonlinear coupling of modes of strings vibrating in two mutually perpendicular directions when there is no obstacle, e.g., the studies of Murthy and Ramakrishna [21] and Elliot [22] to name a few. Murthy and Ramakrishna [21] studied forced vibrations of strings where they found that beyond a critical amplitude of vibration, the string starts oscillating in a perpendicular direction. In another study, Elliot [22] showed that oscillations of strings are generally non-planar and elliptical. The axis of the ellipse is not fixed as well and it precesses due to the nonlinear geometric coupling between the mutually perpendicular transverse modes. The only study on non-planar vibrations with obstacles that the authors are aware of is the one by Vyasarayani et al. [23] where the obstacle is deformable and modeled as distributed viscoelastic springs. However, further details about the work are not available as there has been no follow-up paper of this conference presentation. The main emphasis of this paper is to highlight the role of the nonlinearity due to the wrapping and unwrapping of the string in the development of the higher overtones as well as study the effect of the obstacle on the free vibration characteristics for small amplitude motions. Hence, the complexity of non-planar vibrations has been avoided and it has been left for future work.

In the present work, we have investigated the vibrations of a string against a smooth unilateral obstacle which is placed at one end of the string. We have followed the approach of Vyasarayani et al. [19] for the derivation of the equations of motion and the appropriate boundary conditions which is reported in Section 2. In our formulation we have accounted for all possible effects and accordingly we get some more information about the boundary, in particular, zero velocity of the impending string at the point of separation. We have also presented a dynamic scaling of the spatial domain by which the problem of a linear equation with a moving boundary has been transformed into a nonlinear governing partial differential equation (PDE) in a fixed domain. This scaling helps in properly understanding the nonlinear effects introduced by the moving boundary. In Section 3, we have linearized the governing nonlinear PDE about the static configuration of the string and obtained reduced order model via. Galerkin projection to investigate the natural frequencies and mode shapes of the system. The approximation for the non-trivial shape of the string has been chosen to ensure that all boundary conditions are satisfied. In Section 4, we have obtained reduced order model of the nonlinear equations to study the modal interactions which result in modulations in the amplitudes for the different modes. Results have been obtained for a different number of modes to establish the convergence of the solutions. In Section 5, we present an alternate formulation based on the assumed mode method (AMM) with time-varying polynomial shape functions to verify the results obtained in the previous sections. We note that there is no scaling involved and the formulation accounts for the moving boundary.

2. Mathematical model

A schematic representation of the physical system under consideration has been shown in Fig. 1. It consists of an ideal string (one with no bending stiffness) which vibrates against a smooth parabolic obstacle (the bridge) at one of the ends. The actual sitar string has a portion of the string beyond the bridge as well. However, that portion of the bridge has a very short length compared to the other end and does not contribute much to the dynamics of the longer free portion. Hence it has been neglected and the spatial domain for the string has been assumed to start from the point O which is the point

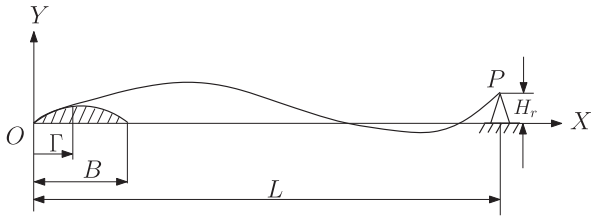

Fig. 1. The simplified physical system for the string vibrations in musical instruments like sitar and veena.

where the bridge starts. The string is under a uniform tension T which has been assumed to be constant during the vibrations and has uniform density ρ per unit length. The assumption of constant tension during vibrations removes the nonlinear effects due to the stretching of the string. Since we are interested in understanding the nonlinear effects due to the presence of the bridge, this is a valid assumption. We note, however, that for large displacements of the string, this effect should be retained. We make two further assumptions related to the motion of the string over the bridge viz.

1. the string perfectly wraps and unwraps around the bridge while going up and down during its motion, respectively and
2. the string remains tangent to the bridge surface at the point of separation ($X=\Gamma$ as shown in Fig. 1).

The first assumption above implies that the contact patch over the bridge is continuous and hence there is only one point of separation. This assumption will not remain valid for large wavenumbers (higher frequencies) where the wavelengths associated with the string displacement become smaller than the extent of the obstacle. For the practical situation of a sitar, this happens around the 50th mode and hence, we claim that the model presented in this paper is only valid for the first few modes (depending on the choice of the parameters), say 20 to be on the conservative side. The second assumption above negates discontinuities in the slopes of the string at the point of separation which are possible for ideal strings. Note that we have assumed a constant tension in the string which trivially satisfies the force continuity within the string. Since penetration of the string inside the bridge is not allowed, there is only one scenario for a slope discontinuity at the point of separation which requires adhesive forces between the string and the bridge which has not been considered in the model. Hence, we disallow any slope discontinuity and assume that the string is in tangential contact with the bridge at the point of separation. The geometry of the bridge is defined by (as in [19])

$$Y_B(X) = A_P X(B-X), \tag{1}$$

where $Y_B(X,t)$ is the height of the bridge, A_P is a constant (related to the curvature of the bridge), and B is the length of the bridge. We will use Hamilton's principle for deriving the equation of motion as well as the boundary condition. This involves minimization of the action integral given by

$$\mathcal{I} = \int_{t_1}^{t_2} \mathcal{L}\, \mathrm{d}t, \tag{2}$$

where $\mathcal{L}$ is the Lagrangian of the system. For our system, the Lagrangian is given by

$$\mathcal{L} = \int_0^L \left[\frac{1}{2}\rho\left(\frac{\partial Y(X,t)}{\partial t}\right)^2 - \frac{1}{2}T\left(\frac{\partial Y(X,t)}{\partial X}\right)^2\right]\mathrm{d}X, \tag{3}$$

where $Y(X,t)$ is the transverse displacement (measured from the X-axis) of an infinitesimal string element of length dX at a distance X from the origin O. However, due to the presence of the obstacle, there exists a geometric constraint at the left boundary which can be identified as

$$Y(X,t) \geq Y_B(X), \quad 0 \leq X \leq B. \tag{4}$$

However, this inequality constraint over a fixed domain can be converted to an equality constraint over a moving domain by introducing $\Gamma(t)$ which is the wrapped length of the string at a given instant of time t and resorting to our previous assumption of a single continuous contact patch. The modified constraint becomes

$$Y(X,t) = Y_B(X), \quad 0 \leq X \leq \Gamma(t), \tag{5}$$

which can also be written in terms of a gap function $G(X,t)$ as

$$G(X,t) = Y(X,t) - Y_B(X) = 0, \quad 0 \leq X \leq \Gamma(t). \tag{6}$$

Notice from the above equality constraint that the solution $Y(X,t)$ for the domain $X \in [0, \Gamma(t)]$ is known and this information can be incorporated in the calculation of the Lagrangian in (3) before substitution in (2) and taking its variation. This will simplify the subsequent variational formulation. We, however, do not follow this approach and proceed with a constrained variational formulation as in [19]. The reason being that we obtain the constraint enforcing force (the Lagrange multiplier) which gives us the distributed normal reaction between the bridge and the string over the contact patch. For the problem studied in this paper, this information is not required but this will be a valuable information while modeling the non-planar vibrations which we plan in future. Finally, substituting (3) into (2) and minimizing subject to the constraint (6) result in the following variational form

$$\begin{aligned}\delta \int_{t_1}^{t_2} \left[\int_0^{\Gamma_-(t)} \left\{\frac{1}{2}\rho\left(\frac{\partial Y(X,t)}{\partial t}\right)^2 - \frac{1}{2}T\left(\frac{\partial Y(X,t)}{\partial X}\right)^2 + \lambda(X)G(X,t)\right\}\mathrm{d}X\right]\mathrm{d}t \\ + \delta \int_{t_1}^{t_2} \left[\int_{\Gamma_+(t)}^{L} \left\{\frac{1}{2}\rho\left(\frac{\partial Y(X,t)}{\partial t}\right)^2 - \frac{1}{2}T\left(\frac{\partial Y(X,t)}{\partial X}\right)^2\right\}\mathrm{d}X\right]\mathrm{d}t = 0,\end{aligned} \tag{7}$$

where $\lambda(X)$ is the Lagrange multiplier (the distributed constraint force). We note that some of the limits of the integrals in (7) are varying with time and hence care has to be taken while interchanging the variational and integral operators.

In particular, there will be a contribution from the variation of the limits of the integral apart from the integrals with the variation of the integrands. The contribution from the variation of the limits can be obtained using Leibniz's integration rule (see [26,27]). Accordingly, we get

$$\int_{t_1}^{t_2}\left[\int_0^{\Gamma_-(t)}\delta\left\{\frac{1}{2}\rho\left(\frac{\partial Y(X,t)}{\partial t}\right)^2-\frac{1}{2}T\left(\frac{\partial Y(X,t)}{\partial X}\right)^2+\lambda(X)G(X,t)\right\}\mathrm{d}X\right]\mathrm{d}t + \int_{t_1}^{t_2}\left[\int_{\Gamma_+(t)}^{L}\delta\left\{\frac{1}{2}\rho\left(\frac{\partial Y(X,t)}{\partial t}\right)^2-\frac{1}{2}T\left(\frac{\partial Y(X,t)}{\partial X}\right)^2\right\}\mathrm{d}X\right]\mathrm{d}t + \int_{t_1}^{t_2}T_1(\Gamma_-(t),t)\delta\Gamma_-(t)\,\mathrm{d}t-\int_{t_1}^{t_2}T_2(\Gamma_+(t),t)\delta\Gamma_+(t)\,\mathrm{d}t=0, \tag{8}$$

where

$$T_1(\Gamma_-(t),t)=\left[\frac{1}{2}\rho\left(\frac{\partial Y(X,t)}{\partial t}\right)^2-\frac{1}{2}T\left(\frac{\partial Y(X,t)}{\partial X}\right)^2+\lambda(X)G(X,t)\right]\Bigg|_{X=\Gamma_-(t)}$$

and

$$T_2(\Gamma_+(t),t)=\left[\frac{1}{2}\rho\left(\frac{\partial Y(X,t)}{\partial t}\right)^2-\frac{1}{2}T\left(\frac{\partial Y(X,t)}{\partial X}\right)^2\right]\Bigg|_{X=\Gamma_+(t)}.$$

The contributions from T_1 and T_2 due to variable boundary were neglected in [19]. Eq. (8) can be reduced to

$$\int_0^{\Gamma_-(t)}\rho\frac{\partial Y(X,t)}{\partial t}\delta Y(X,t)\Big|_{t=t_1}^{t_2}\mathrm{d}X-\int_{t_1}^{t_2}T\left(\frac{\partial Y(X,t)}{\partial X}\right)\delta Y(X,t)\Big|_{X=0}^{\Gamma_-(t)}\mathrm{d}t + \int_{t_1}^{t_2}\int_0^{\Gamma_-(t)}\left[T\frac{\partial^2 Y(X,t)}{\partial X^2}-\rho\frac{\partial^2 Y(X,t)}{\partial t^2}+\lambda(X)\right]\delta Y(X,t)\,\mathrm{d}X\,\mathrm{d}t + \int_{\Gamma_+(t)}^{L}\rho\frac{\partial Y(X,t)}{\partial t}\delta Y(X,t)\Big|_{t=t_1}^{t_2}\mathrm{d}X-\int_{t_1}^{t_2}T\frac{\partial Y(X,t)}{\partial X}\delta Y(X,t)\Big|_{X=\Gamma_+(t)}^{L}\mathrm{d}t + \int_{t_1}^{t_2}\int_{\Gamma_+(t)}^{L}\left[T\frac{\partial^2 Y(X,t)}{\partial X^2}-\rho\frac{\partial^2 Y(X,t)}{\partial t^2}\right]\delta Y(X,t)\,\mathrm{d}X\,\mathrm{d}t + \int_{t_1}^{t_2}[T_1(\Gamma_-(t),t)-T_2(\Gamma_+(t),t)]\delta\Gamma_-(t)\,\mathrm{d}t=0. \tag{9}$$

The first and fourth integrals in (9) are always zero since Y is assumed to be known at t_1 and t_2. Also from the continuity of the string at the point of separation ($X=\Gamma$), we have

$$(a)\delta\Gamma_-(t)=\delta\Gamma_+(t),\quad (b)\delta Y(\Gamma_-(t),t)=\delta Y(\Gamma_+(t),t). \tag{10}$$

Over the wrapped portion of the string, $Y(X,t)=Y_B(X)$ and hence considering a point just to the left to the point of separation ($X=\Gamma_-(t)$), we find that

$$\delta Y(\Gamma_-(t))=A_P(B-2\Gamma_-(t))\delta\Gamma_-(t). \tag{11}$$

Using (10) and (11), (9) can be simplified to

$$\int_{t_1}^{t_2}\left[T_1(\Gamma_-(t),t)-T_2(\Gamma_+(t),t)+T\left(\frac{\partial Y(\Gamma_+(t),t)}{\partial X}-\frac{\partial Y(\Gamma_-(t),t)}{\partial X}\right)A_P(B-2\Gamma_-(t))\right]\delta\Gamma_-(t)\,\mathrm{d}t + \int_{t_1}^{t_2}T\frac{\partial Y(0,t)}{\partial X}\delta Y(0,t)\,\mathrm{d}t+\int_{t_1}^{t_2}\int_0^{\Gamma_-(t)}\left[T\frac{\partial^2 Y(X,t)}{\partial X^2}-\rho\frac{\partial^2 Y(X,t)}{\partial t^2}+\lambda(X)\right]\delta Y(X,t)\,\mathrm{d}X\,\mathrm{d}t - \int_{t_1}^{t_2}T\frac{\partial Y(L,t)}{\partial X}\delta Y(L,t)\,\mathrm{d}t+\int_{t_1}^{t_2}\int_{\Gamma_+(t)}^{L}\left[T\frac{\partial^2 Y(X,t)}{\partial X^2}-\rho\frac{\partial^2 Y(X,t)}{\partial t^2}\right]\delta Y(X,t)\,\mathrm{d}X\,\mathrm{d}t=0. \tag{12}$$

From the above, the equations of motion for the wrapped and free portions are

$$T\frac{\partial^2 Y(X,t)}{\partial X^2}-\rho\frac{\partial^2 Y(X,t)}{\partial t^2}+\lambda(X)=0,\quad 0\le X\le\Gamma_-(t), \tag{13}$$

$$T\frac{\partial^2 Y(X,t)}{\partial X^2}-\rho\frac{\partial^2 Y(X,t)}{\partial t^2}=0,\quad \Gamma_+(t)\le X\le L. \tag{14}$$

The boundary conditions in (12) can be written as

$$(a)\ Y(0,t)=0,\quad (b)\ Y(L,t)=H_r, \tag{15}$$

$$T_1(\Gamma_-(t),t)-T_2(\Gamma_+(t),t)+T\left(\frac{\partial Y(\Gamma_+(t),t)}{\partial X}-\frac{\partial Y(\Gamma_-(t),t)}{\partial X}\right)A_P(B-2\Gamma_-(t))=0. \tag{16}$$

Eq. (16) is called the transversality condition [27]. Now making use of the assumption about slope continuity at the point of separation, i.e.,

$$\frac{\partial Y(\Gamma_-(t),t)}{\partial X}=\frac{\partial Y(\Gamma_+(t),t)}{\partial X}$$

and substituting for T_1 and T_2, we get

$$\left[\frac{1}{2}\rho\left(\frac{\partial Y(X,t)}{\partial t}\right)^2+\lambda(X)G(X,t)\right]\Bigg|_{X=\Gamma_-(t)}-\left[\frac{1}{2}\rho\left(\frac{\partial Y(X,t)}{\partial t}\right)^2\right]\Bigg|_{X=\Gamma_+(t)}=0. \tag{17}$$

Furthermore, the bridge is stationary and since the string perfectly wraps and unwraps around the bridge, the portion of the string over the bridge is stationary as well, i.e., $\partial Y(X,t)/\partial t|_{X=\Gamma_-(t)}=0$. Also $G(\Gamma_-(t),t)=0$ from (6) which simplifies the transversality condition to

$$\frac{\partial Y(\Gamma_+(t),t)}{\partial t}=0. \tag{18}$$

We are interested in the equation of motion for the free portion of the string ($[\Gamma_+,L]$), i.e., (14) since the solution $Y(X,t)$ for the wrapped portion ($[0,\Gamma_-]$), i.e., (13) is known from the geometry of the bridge. At the left boundary ($X=\Gamma_+(t)$) of the free portion of the string, the physical requirement of the continuity of the string gives us

$$Y(\Gamma_+(t),t)=Y_B(\Gamma_-(t))=A_p\Gamma_+(B-\Gamma_+(t)), \tag{19}$$

while the slope continuity results in

$$\frac{\partial Y(\Gamma_+(t),t)}{\partial X}=A_p(B-2\Gamma_+(t)). \tag{20}$$

Next, we notice that differentiation of (19) with respect to t gives

$$\frac{\partial Y(\Gamma_+(t),t)}{\partial X}\frac{\mathrm{d}\Gamma_+(t)}{\mathrm{d}t}+\frac{\partial Y(\Gamma_+(t),t)}{\partial t}=A_p\frac{\mathrm{d}\Gamma_+(t)}{\mathrm{d}t}(B-2\Gamma_+(t)),$$

which reduces to the transversality condition (18) on substitution of $\partial Y(\Gamma_+(t),t)/\partial X$ from (20). Hence, continuity of string (19) coupled with slope continuity at the point of separation (20) leads to the transversality condition (18) thereby making it as a redundant condition. In all subsequent discussions, we will drop the subscript '+' from Γ for ease of notation.

Now we define the nondimensional parameters (following Vyasarayani et al. [19])

$$\bar{x}=\frac{X}{L},\quad \bar{y}(\bar{x},\bar{\tau})=\frac{Y(X,t)}{h},\quad \gamma=\frac{\Gamma(t)}{L},\quad b=\frac{B}{L},\quad \alpha=A_p\frac{L^2}{h},\quad \bar{\tau}=t\sqrt{\frac{T}{\rho L^2}}, \tag{21}$$

where h is any length comparable to the height of the bridge ($A_pB^2/4$). In this paper, we will use h to be the same as the height of the bridge for simplicity. Kindly note from above that we have used different length scales to non-dimensionalize quantities along the X- and the Y-directions. Choosing h to non-dimensionalize Y results in order 1 quantities for the solution $\bar{y}$ and hence, issues related to accuracy of small magnitude solutions during numerical integration are avoided. The choice of L to non-dimensionalize X and Γ along with $\sqrt{T/\rho L^2}$ (which is the typical time scale associated with the string vibrations) to non-dimensionalize t results in a simple form for the governing equation with no parameters. We could have chosen h as the length scale for X and Γ which will result in an extra parameter h/L in the governing equation as well as the boundary conditions. The final results following the procedure outlined in the subsequent discussions remain unchanged with these different choices of length scales in the X-direction. We have preferred L over h since the algebra involved (because of the absence of parameter h/L) is simpler. Further note that this scaling results in a small value for γ and large value for α. However, we will show later that γ can be obtained in closed form and hence smallness of γ as well as largeness of α does not pose any numerical issues.

Using the above nondimensional parameters we rewrite (14) in its nondimensional form as

$$\frac{\partial^2\bar{y}(\bar{x},\bar{\tau})}{\partial\bar{x}^2}-\frac{\partial^2\bar{y}(\bar{x},\bar{\tau})}{\partial\bar{\tau}^2}=0,\quad \gamma\le\bar{x}\le 1. \tag{22}$$

The boundary conditions in the non-dimensional form are

$$\bar{y}(\gamma,\bar{\tau})=\alpha\gamma(b-\gamma),\quad \bar{y}(1,\bar{\tau})=\alpha h_r, \tag{23}$$

and

$$\frac{\partial\bar{y}(\bar{x},\bar{\tau})}{\partial\bar{x}}\Bigg|_{\bar{x}=\gamma}=\alpha(b-2\gamma), \tag{24}$$

where $\alpha h_r = H_r/h$. Next we rescale the spatial domain as $x = (\overline{x}-\gamma)/(1-\gamma)$ and time domain as $\tau = \overline{\tau}$ so that $\overline{y}(\overline{x},\overline{\tau}) = y(x,\tau)$. With this rescaling, the spatial domain becomes fixed to $x \in [0,1]$ and hence the complexity of the moving boundary is avoided. The derivatives in the new variables x and τ are related to the derivatives in the old variables $\overline{x}$ and $\overline{\tau}$. These relations are given by

$$\frac{\partial \overline{y}(\overline{x},\overline{\tau})}{\partial \overline{\tau}} = \frac{\partial y(x,\tau)}{\partial x}\frac{\partial x}{\partial \overline{\tau}} + \frac{\partial y(x,\tau)}{\partial \tau}\frac{\partial \tau}{\partial \overline{\tau}}, \tag{25}$$

and

$$\frac{\partial \overline{y}(\overline{x},\overline{\tau})}{\partial \overline{x}} = \frac{\partial y(x,\tau)}{\partial x}\frac{\partial x}{\partial \overline{x}} + \frac{\partial y(x,\tau)}{\partial \tau}\frac{\partial \tau}{\partial \overline{x}}, \tag{26}$$

where

$$\frac{\partial x}{\partial \overline{\tau}} = \frac{(\overline{x}-1)}{(1-\gamma)^2}\dot{\gamma} = \frac{(x-1)}{(1-\gamma)}\dot{\gamma}, \quad \frac{\partial \tau}{\partial \overline{\tau}} = 1, \quad \frac{\partial x}{\partial \overline{x}} = \frac{1}{(1-\gamma)}, \quad \frac{\partial \tau}{\partial \overline{x}} = 0. \tag{27}$$

Using (25)–(27), we get the double derivatives

$$\frac{\partial^2 \overline{y}(\overline{x},\overline{\tau})}{\partial \overline{\tau}^2} = \left[\frac{(x-1)^2\dot{\gamma}^2}{(1-\gamma)^2}\right]\frac{\partial^2 y(x,\tau)}{\partial x^2} + \left[\frac{(x-1)}{(1-\gamma)}\left(\frac{2\dot{\gamma}^2}{(1-\gamma)} + \ddot{\gamma}\right)\right]\frac{\partial y(x,\tau)}{\partial x} + \left[2\frac{(x-1)\dot{\gamma}}{(1-\gamma)}\right]\frac{\partial^2 y(x,\tau)}{\partial x \partial \tau} + \frac{\partial^2 y(x,\tau)}{\partial \tau^2}. \tag{28}$$

and

$$\frac{\partial^2 \overline{y}(\overline{x},\overline{\tau})}{\partial \overline{x}^2} = \frac{1}{(1-\gamma)^2}\frac{\partial^2 y(x,\tau)}{\partial x^2}. \tag{29}$$

Substituting (28) and (29) into (22) gives us

$$\left[\frac{(x-1)^2\dot{\gamma}^2 - 1}{(1-\gamma)^2}\right]\frac{\partial^2 y}{\partial x^2} + \left[\frac{(x-1)}{(1-\gamma)}\left(\frac{2\dot{\gamma}^2}{(1-\gamma)} + \ddot{\gamma}\right)\right]\frac{\partial y}{\partial x} + \left[\frac{2(x-1)\dot{\gamma}}{(1-\gamma)}\right]\frac{\partial^2 y}{\partial x \partial \tau} + \frac{\partial^2 y}{\partial \tau^2} = 0. \tag{30}$$

where for brevity we have dropped the explicit dependence of y on the variables x and τ. The boundary conditions (23) and (24) in the rescaled variables can be rewritten as

$$y(0,\tau) = \alpha\gamma(b-\gamma), \quad y(1,\tau) = \alpha h_r, \tag{31}$$

and

$$\left.\frac{\partial y(x,\tau)}{\partial x}\right|_{x=0} = \alpha(b-2\gamma)(1-\gamma). \tag{32}$$

Equation of motion (30) is a nonlinear equation where γ is another state variable which is related to the dependent variable y by the relation expressed in (32). Eqs. (30)–(32) complete the mathematical formulation for our system.

3. Linearization to study natural frequencies and modeshapes

In this section, we linearize the nonlinear equation of motion (30) about the static configuration of the string which itself is derived here so as to study the linear vibration characteristics of our system. To this end, we assume that

$$y(x,t) = y_{st}(x) + \epsilon\tilde{y}(x,\tau), \tag{33}$$

and

$$\gamma = \gamma_{st} + \epsilon\tilde{\gamma}(\tau), \tag{34}$$

where $0 < \epsilon \ll 1$, $y_{st}(x)$ is the static configuration of the string, and γ_{st} is the length of the wrapped portion of the string in the static configuration. We substitute (33) and (34) into (30), expand it in a Taylor series about $\epsilon = 0$ and collect terms of various orders of ϵ to get the equation governing the static equilibrium (at order 1) and the linearized equation of motion (at order ϵ) as

$$\left[\frac{1}{(1-\gamma_{st})^2}\right]\frac{\partial^2 y_{st}}{\partial x^2} = 0, \tag{35}$$

and

$$\frac{\partial^2 \tilde{y}(x,\tau)}{\partial \tau^2} - \frac{1}{(1-\gamma_{st})^2}\frac{\partial^2 \tilde{y}(x,t)}{\partial x^2} - \frac{(1-x)}{(1-\gamma_{st})}\frac{dy_{st}(x)}{dx}\frac{d^2\tilde{\gamma}}{d\tau^2} - \frac{2\tilde{\gamma}}{(1-\gamma_{st})^3}\frac{d^2 y_{st}(x)}{dx^2} = 0, \tag{36}$$

respectively. Next a substitution of (33) and (34) into the boundary conditions (31) and equating different order terms of ϵ to zero leads to

$$y_{st}(0,\tau)=\alpha\gamma_{st}(b-\gamma_{st}),\quad \tilde{y}(0,\tau)=\alpha(b-2\gamma_{st})\tilde{\gamma}(\tau),\quad y_{st}(1,\tau)=\alpha h_r,\quad \tilde{y}(1,\tau)=0. \tag{37}$$

The static configuration of the string (from (35) and (37)) is

$$y_{st}(x)=\alpha\gamma_{st}(b-\gamma_{st})(1-x)+\alpha h_r x, \tag{38}$$

where γ_{st} is yet undetermined. To obtain the equation for γ_{st}, we substitute (33) and (34) along with (38) in (32) and separate terms of different orders of ϵ. At order 1, we have

$$\gamma_{st}^2-2\gamma_{st}+b-h_r=0, \tag{39}$$

which upon gives us[1]

$$\gamma_{st}=1-\sqrt{1+h_r-b}. \tag{40}$$

The order ϵ equation gives a relation between $\tilde{\gamma}$ and $\tilde{y}$

$$\left.\frac{\partial\tilde{y}}{\partial x}\right|_{x=0}=-\alpha\tilde{\gamma}\left(b-4\gamma_{st}+2\right). \tag{41}$$

Finally, we substitute (38) into (36) to get the simplified linearized equation

$$\frac{\partial^2\tilde{y}(x,\tau)}{\partial\tau^2}+\alpha\left[\gamma_{st}(b-\gamma_{st})-h_r\right]\frac{(1-x)}{(1-\gamma_{st})}\frac{\mathrm{d}^2\tilde{\gamma}}{\mathrm{d}\tau^2}-\frac{1}{(1-\gamma_{st})^2}\frac{\partial^2\tilde{y}(x,t)}{\partial x^2}=0. \tag{42}$$

3.1. Natural frequencies

Proceeding forward, we assume

$$\tilde{y}=\alpha(b-2\gamma_{st})\tilde{\gamma}(1-x)+\sum_{n=1}^{\infty}\beta_n(t)\sin(n\pi x) \tag{43}$$

which satisfies the boundary conditions for $\tilde{y}$ given in (37). Substitution of (43) into (41) gives us $\tilde{\gamma}$ as

$$\tilde{\gamma}=-\frac{1}{2\alpha(1-\gamma_{st})}\sum_{n=1}^{\infty}n\pi\beta_n(t). \tag{44}$$

For the study of vibration characteristics of our system, we substitute (43) and (44) into (42) to obtain

$$\sum_{n=1}^{\infty}\ddot{\beta}_n(t)\ \sin(n\pi x)-\frac{(b-2\gamma_{st}+\gamma_{st}^2-h_r)(1-x)}{2(1-\gamma_{st})^2}\sum_{n=1}^{\infty}n\pi\ddot{\beta}_n(t)$$
$$+\frac{1}{(1-\gamma_{st})}\sum_{n=1}^{\infty}n^2\pi^2\beta_n(t)\ \sin(n\pi x)=0. \tag{45}$$

The second term of (45) becomes zero from (39). As a result, the Galerkin projection wherein (45) is multiplied with $\sin(m\pi x)$ and integrated over the x domain, i.e., $x\in[0,\ 1]$ results in decoupled ordinary differential equations (ODEs) for the various β_m as

$$\ddot{\beta}_m(t)+\frac{m^2\pi^2}{(1-\gamma_{st})^2}\beta_m(t)=0,\quad \text{for } m=1,2,\ldots,\infty. \tag{46}$$

Hence, the natural frequencies for our system are $(m\pi/(1-\gamma_{st}))$ and they are harmonic. The overall effect of the finite-sized bridge is to alter the frequencies by altering the static wrapped length (γ_{st}) of the string. Since a static smooth obstacle as considered in our current model does not introduce any inharmonicity in the system which can counter the inharmonicity introduced by the bending stiffness of the strings, our model cannot explain the observation about the harmonic nature of the musical instruments used in Indian classical music. However, as will be shown later, it does explain the modulations as well as the appearance of the higher overtones which is predominantly observed in the instruments used in Indian classical music. Initially, it seems that our results are in contrast to the experimental findings of Valette et al. [12] who observed a significant dispersion and inharmonicity for a string vibrating against a curved obstacle. However, we note that the experiments reported in [12] were for a tanpura with the 'juari' that introduces a non-smoothness in the bridge profile. As a result, smooth wrapping and unwrapping are prohibited and discontinuous changes in γ and impacts are inevitable during the motion. These impacts result in the dispersion for Valette et al. [12] and are not present in our model since we have considered a smooth bridge geometry. Hence, there is no contradiction between our results and those of Valette et al. [12]. Another interesting observation about the natural frequencies in our model is that they do not depend on the curvature of the bridge (α). In contrast, experienced

[1] The other root $1+\sqrt{1+h_r-b}>1$ is not feasible.

craftsmen of these musical instruments emphasize the need for a specific curvature and this effect will probably come into play in the non-planar oscillations of the strings as well as coupled plate–string vibrations which have not been considered in this work. However, the details of the curved bridge geometry play an instrumental role in determining the exchange of energy between the various string modes through modal interactions to be presented in Section 4.

3.2. Mode shapes

Finally, we focus on the mode-shapes associated with the natural frequencies. For this, we substitute (44) and (43) to get

$$\tilde{y} = \sum_{n=1}^{\infty} \beta_n(t)\left[\sin(n\pi x) - n\pi\frac{(b-2\gamma_{st})}{2(1-\gamma_{st})}(1-x)\right]. \tag{47}$$

Therefore, the mode-shapes are given by

$$\sin(n\pi x) - n\pi\frac{(b-2\gamma_{st})}{2(1-\gamma_{st})}(1-x), \tag{48}$$

where $n = 1, 2, \ldots, \infty$. Here we note that $x = (\bar{x}-\gamma)/(1-\gamma)$ where γ is a function of time making the mode shapes in the unscaled spatial variable $\bar{x}$ as time dependent. At this point, we note that our mode shapes do not strictly follow the separation of time and space variables in the real domain even though they do so in the scaled domain. However, all the material points on the string for this time-varying functional representation of the displacement have synchronous motion with the same frequency and this representation gives the relative amplitude of the displacement of the various material points on the string. Hence, this representation is also referred to as a time-varying mode-shape. Using (47) and (38) the solution $y = y_{st} + \epsilon\tilde{y}$ for the nth modeshape of the string in the unscaled domain can be written as

$$\bar{y}_n = \alpha\gamma_{st}(b-\gamma_{st})\frac{(1-\bar{x})}{(1-\gamma_n)} + \alpha h_r\frac{(\bar{x}-\gamma_n)}{(1-\gamma_n)} + \epsilon\beta_n\left[\sin\left(n\pi\frac{(1-\bar{x})}{(1-\gamma_n)}\right) - n\pi\frac{(b-2\gamma_{st})(1-\bar{x})}{2(1-\gamma_{st})(1-\gamma_n)}\right], \tag{49}$$

where

$$\gamma_n = \gamma_{st} - \epsilon\frac{n\pi\beta_n}{2\alpha(1-\gamma_{st})}, \tag{50}$$

and $\gamma_{st} = 1 - \sqrt{1+h_r-b}$. For higher modes with large values of n, the corresponding value of β_n reduces to ensure that $\epsilon\tilde{y}(x,\tau) \ll y_{st}$ and $\epsilon\tilde{\gamma} \ll \gamma_{st}$ so that the ordering of the terms is not violated. We note from the above that γ_n depends on β_n and hence the mode-shapes are dependent on the amplitude of the solution as well. Larger the initial amplitude, larger is the variation in the mode-shapes with time. This is depicted in Figs. 2 and 3 where the string configurations at different time instants have been plotted for the second and third modes, respectively for $h_r = 0$, $b = 0.05$, and $\alpha = 4/b^2$. Note that the shapes for the string plotted in Figs. 2 and 3 are overly exaggerated (by choosing large values for β_2 and β_3) to show the variations. The actual shape of the string remains close to a straight line during the actual vibrations. An important thing to notice from these figures is that the crossing of the string with its static (green) configuration (a node for the mode-shape) is not a fixed point but changes with time. The nodal points move along the static configuration of the string with time which probably can be understood as the cause of modulation in the frequency of the sound of musical instruments, and the non-stationary nodal points explain the non-applicability of the Young–Helmholtz law which is valid for situations with fixed nodal points. Similar observations for the nodal points have been reported in [20] even though not explicitly mentioned.

An advantage of our results is that we can analytically estimate the change in the nodal points by solving (48) using a regular perturbation method which provides useful information about possible overlaps between the nodal points for

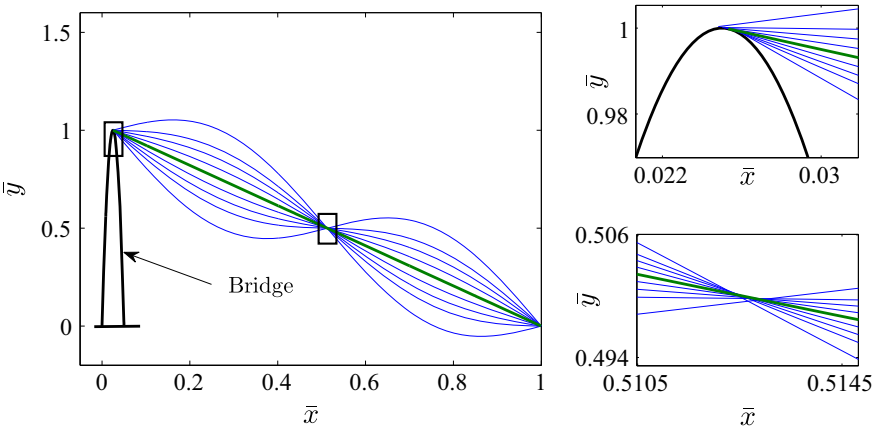

Fig. 2. Left: configuration of the string while vibrating in second mode. Right: a magnified view of the boxed portion from the left.

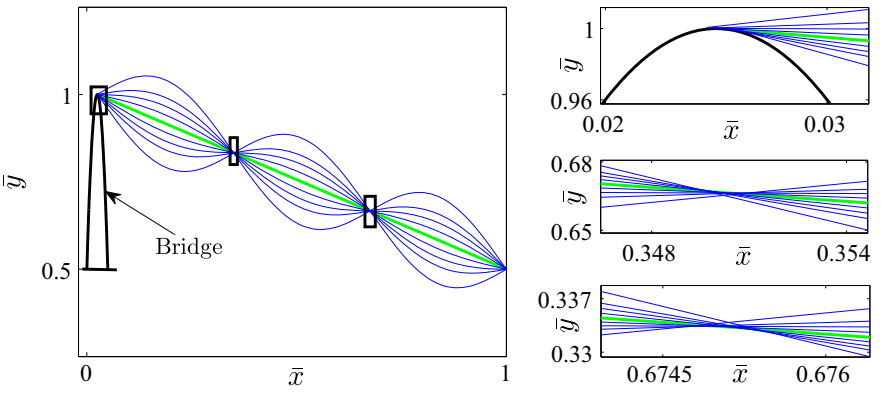

Fig. 3. Left: configuration of the string while vibrating in third mode. Right: magnified views of the boxed portions from the left.

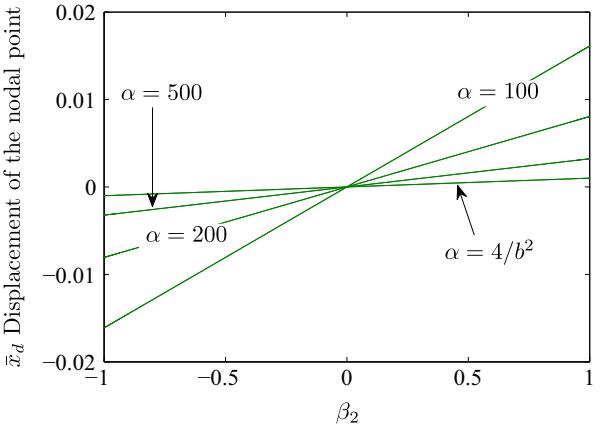

Fig. 4. Displacement of the nodal point of the second mode.

different modes and the resulting interactions. To this end, we first write the mode shapes given in (48) in terms of the unscaled spatial domain $\bar{x}$ by substituting $x=(\bar{x}-\gamma)/(1-\gamma)$, which results in

$$\sin\left(n\pi\frac{(1-\bar{x})}{(1-\gamma)}\right)+\mu n\frac{(1-\bar{x})}{(1-\gamma)}=0, \tag{51}$$

where $\mu=\pi(2\gamma_{\rm st}-b)/2(1-\gamma_{\rm st})\ll 1$ is a small positive quantity. We substitute $\bar{x}=\bar{x}_0+\mu\bar{x}_1$ and $\gamma=\gamma_{\rm st}+\mu\tilde{\gamma}$ into (51). Then separating terms of order 1 and μ and setting them to zero individually, we obtain

$$\sin\left(n\pi\frac{(\bar{x}_0-\gamma_{\rm st})}{(1-\gamma_{\rm st})}\right)=0, \tag{52}$$

$$\pi\left[(\bar{x}_1-\tilde{\gamma})+\frac{(\bar{x}_0-\gamma_{\rm st})}{(1-\gamma_{\rm st})}\tilde{\gamma}\right]\cos\left(n\pi\frac{(\bar{x}_0-\gamma_{\rm st})}{(1-\gamma_{\rm st})}\right)+(1-\bar{x}_0)=0. \tag{53}$$

Solving (52) and (53) for $\bar{x}_0$ and $\bar{x}_1$ we get

$$\bar{x}_0=(1-\gamma_{\rm st})\frac{m}{n}+\gamma_{\rm st}, \tag{54}$$

$$\bar{x}_1=\left(\frac{1-\bar{x}_0}{1-\gamma_{\rm st}}\right)\tilde{\gamma}-\frac{1-\bar{x}_0}{\pi\cos\left(\dfrac{n\pi(\bar{x}_0-\gamma_{\rm st})}{(1-\gamma_{\rm st})}\right)}, \tag{55}$$

where $0\le m\le n$ is another integer ($m=0$ and n are the two end points of the string). Using solutions (54) and (55) and the relation (50) for $\tilde{\gamma}_n$, the location of the nodal point $\bar{x}=\bar{x}_0+\mu\bar{x}_1$ can be written as

$$\bar{x}=(1-\gamma_{\rm st})\frac{m}{n}+\gamma_{\rm st}-\mu\frac{(n-m)(1-\gamma_{\rm st})}{n\pi\cos(m\pi)}-\mu\frac{\pi(n-m)\beta_n}{2\alpha(1-\gamma_{\rm st})} \tag{56}$$

We numerically solved (51) and compared our results with the analytical solution (56) which match to the seventh decimal place for the parameters reported earlier in this section. From the analytical expression for the nodal points (56), we clearly

observe that it has a static part which denotes the mean position of the node due to the obstacle and a dynamic part (the term dependent on β_n which changes with time) which is the measure of the movement of the nodal point along the $\bar{x}$-axis. The dynamic component $\mu\bar{x}_d = \mu(\pi(n-m)\beta_n/2\alpha(1-\gamma_{st}))$ depends on α which represents the curvature of the bridge. As the curvature (α) reduces down which means the bridge becomes flatter then the nodal point moves more from its mean position as depicted for the displacement ($\bar{x}_d$) of the nodal point from its mean position for the second mode in Fig. 4. For practical situations, the curvature of the bridge is very small and hence, there is a significant movement of the nodal points expected for the various modes.

4. Modal interactions

In the previous sections, we have investigated the natural frequencies and mode-shapes of the system which are associated with the linearization of the equation of motion about its static configuration. In this section, we will reduce the nonlinear PDE (30) to a set of nonlinear ODE's using the Galerkin projection method and numerically investigate their response to better understand the interactions among the various modes. We assume a solution of the form

$$y(x,\tau) = \alpha\gamma(b-\gamma)(1-x) + \alpha h_r x + \sum_{n=1}^{N} \beta_n(\tau)\ \sin(n\pi x) \tag{57}$$

to (30) which satisfies the boundary conditions (31). Satisfying the slope continuity boundary condition (32) at $x=0$ with (57), we get the relation

$$\gamma^2 - 2\gamma + b - h_r - \frac{1}{\alpha}\sum_{n=1}^{N} n\pi\beta_n = 0. \tag{58}$$

The only possible solution to (58) is given by

$$\gamma = 1 - \sqrt{1 - b + h_r + \frac{1}{\alpha}\sum_{n=1}^{N} n\pi\beta_n(\tau)}. \tag{59}$$

Accordingly, we have

$$\dot{\gamma} = -\frac{1}{2\alpha(1-\gamma)}\sum_{n=1}^{N} n\pi\dot{\beta}_n(\tau), \tag{60}$$

and

$$\ddot{\gamma} = \frac{\dot{\gamma}^2}{(1-\gamma)} - \frac{1}{2\alpha(1-\gamma)}\sum_{n=1}^{N} n\pi\ddot{\beta}_n(\tau). \tag{61}$$

We substitute (57) followed by (59)–(61) into (30) and apply the Galerkin projection technique with the modes $\sin(m\pi x)$ to get the following nonlinear ODEs for the evolution of the various β_ms':

$$\begin{aligned}
&\sum_{n=1}^{N}\left[K_{2nm} - \frac{n\pi}{2\alpha(1-\gamma)^2}\left[\sum_{p=1}^{N} p\pi\beta_p K_{4pm} - \alpha(b-2\gamma+\gamma^2-h_r)K_{3m}\right]\right]\ddot{\beta}_n \\
&+\frac{\dot{\gamma}^2}{(1-\gamma)^2}\left[\sum_{n=1}^{N} n\pi(3K_{4nm} - n\pi K_{1nm})\beta_n + \alpha(2-3b+2\gamma-\gamma^2+3h_r)K_{3m}\right] \\
&+\frac{2\dot{\gamma}}{(1-\gamma)}\sum_{n=1}^{N} n\pi\dot{\beta}_n K_{4nm} + \frac{1}{(1-\gamma)^2}\sum_{n=1}^{N} n^2\pi^2\beta_n K_{2nm} = 0,
\end{aligned} \tag{62}$$

where $m = 1, 2, \ldots N$ and the Ks' are defined as

$$K_{1nm} = \int_0^1 (x-1)^2\ \sin(n\pi x)\ \sin(m\pi x)\,\mathrm{d}x = \begin{cases} \dfrac{4nm}{(n^2-m^2)^2\pi^2} & \text{if } n \neq m, \\ \left(\dfrac{1}{6} - \dfrac{1}{4n^2\pi^2}\right) & \text{if } n = m, \end{cases}$$

$$K_{2nm} = \int_0^1 \sin(n\pi x)\ \sin(m\pi x)\,\mathrm{d}x = \frac{1}{2}\delta_{nm},$$

$$K_{3m} = \int_0^1 (x-1)\ \sin(m\pi x)\,\mathrm{d}x = -\frac{1}{m\pi},$$

$$K_{4nm} = \int_0^1 (x-1)\ \cos(n\pi x)\ \sin(m\pi x)\,\mathrm{d}x = \begin{cases} \dfrac{m}{(n^2-m^2)\pi} & \text{if } n \neq m, \\ -\dfrac{1}{4n\pi} & \text{if } n = m. \end{cases}$$

For simplicity of representation, we have not replaced γ and $\dot{\gamma}$ in (62) by their corresponding expressions in terms of β_n's and $\dot{\beta}_n$'s reported in (59) and (60). However, this substitution results in system of equations purely in terms of β_n's. This system

of equations obtained after some algebraic manipulations is

$$\sum_{n=1}^{N}\left[K_{2nm}\left(1-b+h_r+\frac{1}{\alpha}\sum_{p=1}^{N}p\pi\beta_p\right)-\frac{n\pi}{2\alpha}\sum_{p=1}^{N}p\pi\beta_p(K_{4pm}-K_{3m})\right]\ddot{\beta}_n + \frac{\left(\sum_{p=1}^{N}p\pi\dot{\beta}_p\right)^2}{4\alpha^2\left(1-b+h_r+\frac{1}{\alpha}\sum_{p=1}^{N}p\pi\beta_p\right)}\left[\sum_{n=1}^{N}n\pi(3K_{4nm}-n\pi K_{1nm}-K_{3m})\beta_n-2\alpha(b-h_r-1)K_{3m}\right] -\frac{1}{\alpha}\sum_{p=1}^{N}p\pi\dot{\beta}_p\sum_{n=1}^{N}n\pi\dot{\beta}_nK_{4nm}+\sum_{n=1}^{N}n^2\pi^2\beta_nK_{2nm}=0. \quad (63)$$

We solve the set of equations represented by (63) numerically using the Matlab ODE solver ode45 with a tolerance of 10^{-6} and have reported the results for $b=0.05, \alpha=4/b^2$ and $h_r=0$ (following [19]). Amplitude plots for the modal coordinates corresponding to the first three modes are shown in Fig. 5 where we have used the initial condition $\beta_1(0)=2$ with the initial condition for the other modes as zero. It can be easily observed from Fig. 5 that the amplitude corresponding to the various modes has some modulation with time. Also note that even though we start our simulations with the first mode only, the amplitudes corresponding to the higher modes gradually pick-up and start appearing in the long-term solution. We note that there is no dissipation in our system and hence, convergence is not truly obtained in the strict sense. Energy exchange among the various modes due to modal interactions results in a statistical equipartition of energy between the various modes over long times. Hence, the energy contained in the various modes changes with a change in the number of modes used in the Galerkin truncation which modifies the modulation patterns observed for the modal coordinates. However, for large N, the change in the energy content in the existing modes by the introduction of a few new modes is not very significant and hence, the qualitative nature of the modulations remains the same. Hence, a weak sense of convergence can be identified wherein the qualitative nature of the modulations does not change with increasing N. We also emphasize that the main objective of this section is to demonstrate the presence of amplitude modulations and appearance of higher modes in our model with smooth wrapping and unwrapping similar to the ones observed in experiments, and hence the issue of convergence is not very critical. In real scenario, there is some dissipation mechanism in the system which damps the higher modes much faster and ensures a value of N for the truncation corresponding to convergence. We further note that it has been shown in [24,25] that truncation applied to problems involving moving strings can lead to erroneous results especially under situations corresponding to parametric resonance. However, since our system of Eq. (63) is an autonomous system, there is no possibility of such a scenario.

We next focus on the solution corresponding to the first three modes with increasing number of modes in our approximation to study the convergence of the solutions in the sense outlined above. For this study, we have used only one initial condition, i.e., $\beta_1(0)=2, \beta_n(0)=0$ and $\dot{\beta}_m(0)=0$ where $n=2,3,\ldots,N$ and $m=1,2,\ldots,N$. Figs. 6–8 show the variations in the amplitudes β_1, β_2, and β_3 respectively for different number of modes (N) accommodated in the approximation. These figures show that for smaller N, the modulation pattern in the amplitudes changes with the increase in number of modes (N), but around $N=16$, the modulation patterns in these three modes have converged. The convergence of the solution in the

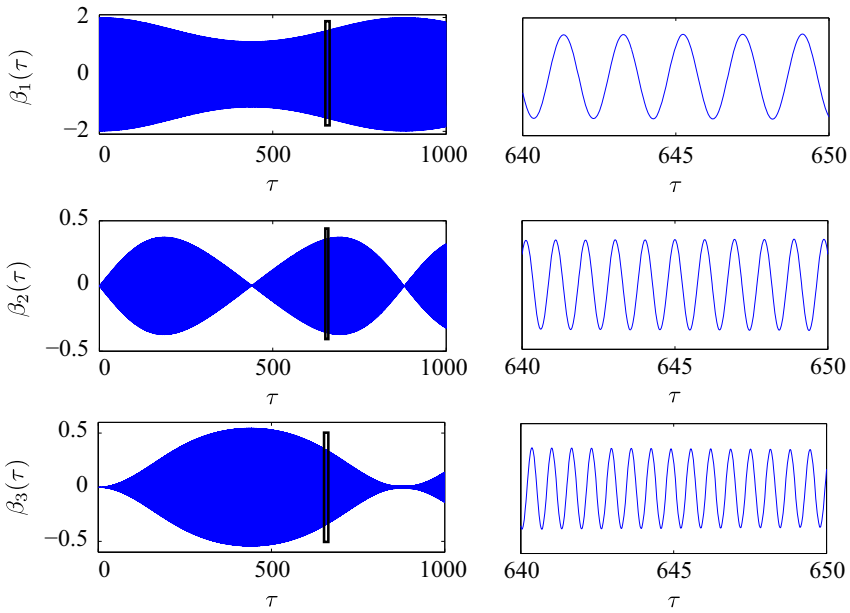

Fig. 5. Left: amplitude plots for $N=3$. Right: a magnified view of the boxed portion from the left.

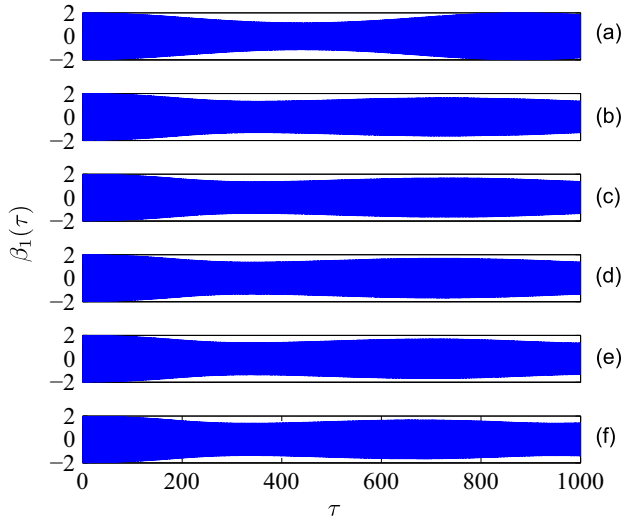

Fig. 6. Amplitude plot of $\beta_1(\tau)$ for $N=3$ (a) , 10 (b), 12 (c), 14 (d), 16 (e), 18 (f).

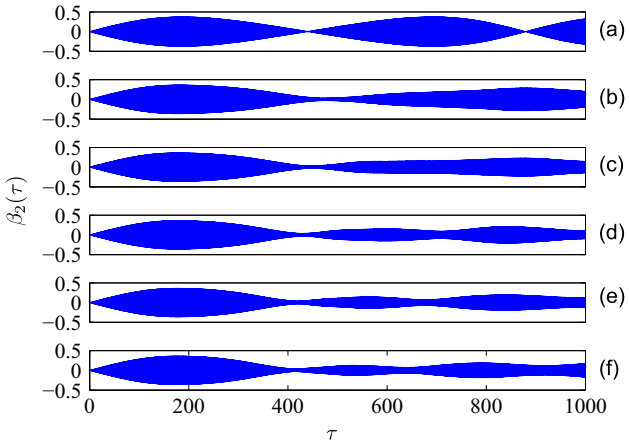

Fig. 7. Amplitude plot of $\beta_2(\tau)$ for $N=3$ (a), 10 (b), 12 (c), 14 (d), 16 (e), 18 (f).

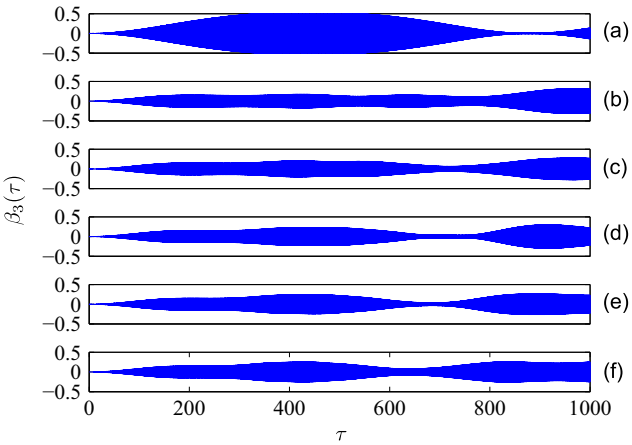

Fig. 8. Amplitude plot of $\beta_3(\tau)$ for $N=3$ (a), 10 (b), 12 (c), 14 (d), 16 (e), 18 (f).

weak sense is further established by considering variations in global quantities like the contact length (γ), the kinetic and potential energy of the entire system with time. Since these quantities do not depend on a specific mode, modulation patterns in these quantities are a better indicator of convergence. Figs. 9–11 depict the time variation of the contact length of

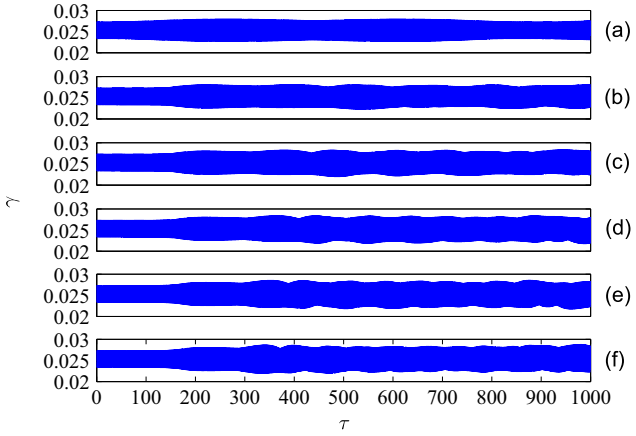

Fig. 9. Contact length γ for $N=3$ (a), 10 (b), 12 (c), 14 (d), 16 (e), 18 (f) .

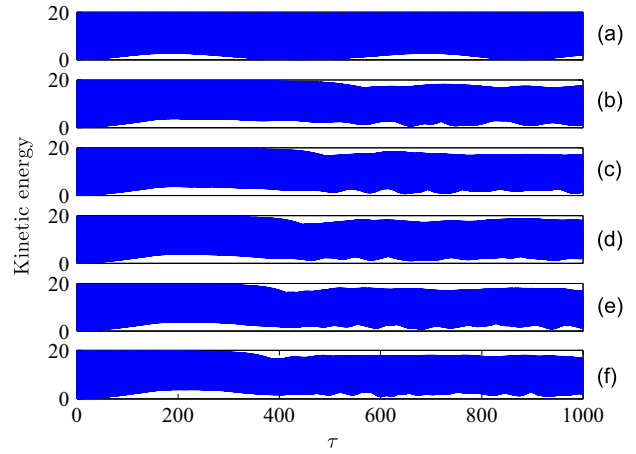

Fig. 10. Kinetic energy for $N=3$ (a), 10 (b), 12 (c), 14 (d), 16 (e), 18 (f).

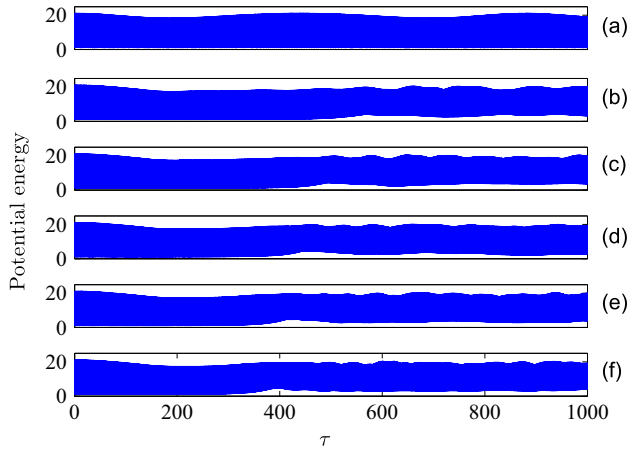

Fig. 11. Potential energy for $N=3$ (a), 10 (b), 12 (c), 14 (d), 16 (e), 18 (f).

the string over the bridge, the total kinetic energy and the total potential energy for a different number of modes used for the approximation. For each of these quantities, we can observe that the modulation patterns for $N=16$ and $N=18$ are nearly the same indicating that the solutions have converged in the weak sense mentioned previously. Another interesting point to observe from these figures is that the variation in the kinetic and potential energies is anti-correlated since the total energy is conserved due to the impending zero velocity at the point of separation in our model.

We finally note that the system of equations represented by (63) also depends on the parameter h_r. We have performed the parametric study of the solutions with changes in h_r but observed that the variation in the value of h_r just changes the frequency of the solutions by modifying the contact length for the static configuration γ_{st} but does not change the qualitative behavior of the solutions. Hence, these results have not been reported in this paper.

5. Verification of results with the assumed mode method

In the previous sections, we have studied linear and nonlinear behavior of the system using the Galerkin projection technique on the scaled system of equations with the boundary conditions obtained using Hamilton's principle. In this section, we obtain the equations of motion for our system directly without any scaling of the spatial domain using a different approach that we will refer as the assumed mode method (AMM). In this method, we first assume a displacement field for the string in the non-dimensional form which satisfies the continuity of the string as well as the slope continuity at the point of separation viz. (23) and (24). The Lagrangian of the system is obtained in terms of this assumed solution for the string displacement which gives it in terms of finitely many generalized coordinates. The evolution of these generalized coordinates is then obtained using the Euler–Lagrange equations. To maintain diversity in the solutions, time-varying polynomial shape functions have been used to represent the string displacement in this approach as opposed to the Sine series in the Galerkin projection approach. For simplification, we are reporting the derivation for the case with $H_r=0$ for which results have already been reported in the previous sections.

There is no restriction on the properties of the functions used for the AMM except that they should be chosen such that the assumed displacement of the string satisfies the displacement and slope continuity at the point of separation. We note that a choice of orthogonal functions will result in better convergence properties for the AMM. However, for the purpose of verifying the obtained results from the Galerkin approach, this issue is not very critical. Accordingly, we chose the simplest polynomial representation satisfying the slope and displacement continuity and represent the non-dimensional displacement for the free portion of the string as

$$\overline{y} = c_1\overline{x}^2 + c_2\overline{x} + c_3 + \beta_1(t)(\overline{x}-1)(\overline{x}-\gamma)^2 + \sum_{n=2}^{N}\beta_n(t)(\overline{x}-1)(\overline{x}-\gamma)^2\prod_{k=1}^{n-1}\left(\overline{x}-\frac{k}{n}(1-\gamma)\right), \tag{64}$$

where c_1, c_2 and c_3 are functions of γ. These coefficients are uniquely determined in terms of the contact length of the string γ to make our assumed solution satisfy the conditions (23) and (24). This solution is given by

$$c_1 = -\frac{\alpha(\gamma^2-2\gamma+b)}{(1-\gamma^2)}, \quad c_2 = \frac{\alpha(\gamma^2 b-2\gamma+b)}{(1-\gamma^2)}, \quad c_3 = \frac{\alpha\gamma^2(1-b)}{(1-\gamma^2)}. \tag{65}$$

Accordingly, the generalized coordinates for our AMM are γ and β_n, $n=1,2,\ldots,N$. The Lagrangian of our system with this assumed displacement field can be written as

$$\mathcal{L} = \int_{\overline{x}=0}^{\gamma} -\frac{1}{2}\left(\frac{\partial y_b}{\partial\overline{x}}\right)^2 \mathrm{d}\overline{x} + \int_{\overline{x}=\gamma}^{1}\left[\frac{1}{2}\left(\frac{\partial\overline{y}}{\partial\overline{\tau}}\right)^2 - \frac{1}{2}\left(\frac{\partial\overline{y}}{\partial\overline{x}}\right)^2\right]\mathrm{d}\overline{x}, \tag{66}$$

where $y_b = Y_B(X)/h$ is the non-dimensional function representing the bridge geometry. The kinetic energy of the wrapped portion of the string is considered to be zero since the bridge is static. The Euler–Lagrange equations of motion in terms of the generalized coordinates are given by

$$\frac{\mathrm{d}}{\mathrm{d}\overline{\tau}}\left(\frac{\partial\mathcal{L}}{\partial\dot{\gamma}}\right) - \frac{\partial\mathcal{L}}{\partial\gamma} = 0, \tag{67}$$

and

$$\frac{\mathrm{d}}{\mathrm{d}\overline{\tau}}\left(\frac{\partial\mathcal{L}}{\partial\dot{\beta}_n}\right) - \frac{\partial\mathcal{L}}{\partial\beta_n} = 0, \tag{68}$$

for $n=1,2,\ldots,N$. Eqs. (67) and (68) are $N+1$ coupled nonlinear ODEs which represent the system of equations for our physical model under the AMM.

5.1. Linear analysis

As in the previous sections, we start with a study of the linearized equations for which we substitute $\gamma=\gamma_{st}+\epsilon\tilde{\gamma}(\overline{\tau})$ and $\beta_n=\beta_{n,st}+\epsilon\tilde{\beta}_n(\overline{\tau})$ into (67) and (68) with γ_{st} and $\beta_{n,st}$ representing the coordinates at the static configuration. The terms of order 1 give us N nonlinear algebraic equations for γ_{st} and $\beta_{n,st}$ which are solved numerically. All terms which are of order ϵ give us the linearized equations for $\ddot{\tilde{\gamma}}$ and $\ddot{\tilde{\beta}}_n$'s which can be written in the following form

$$[\mathbf{M}]\{\ddot{\xi}\} + [\mathbf{S}]\{\xi\} = 0, \tag{69}$$

where $\{\xi\} = \{\tilde{\gamma}, \tilde{\beta}_1, \tilde{\beta}_2, \ldots\tilde{\beta}_N\}'$ and the entries of the matrix $[\mathbf{M}]$ and $[\mathbf{S}]$ depend on the coordinates at the static configuration. The eigenvalues of $[\mathbf{M}]^{-1}[\mathbf{S}]$ are squares of the natural frequencies of the system. Natural frequencies obtained from (46)

Table 1
Natural frequencies for two different approaches.

Method	Natural frequencies						
	1st	2nd	3rd	4th	5th	6th	7th
AMM ($N=3$)	3.22322	6.44830	10.36849	14.52759	–	–	–
AMM ($N=4$)	3.22321	6.44830	9.68849	14.52759	19.22051	–	–
AMM ($N=5$)	3.22321	6.44642	9.68849	12.97739	19.22051	24.50626	–
AMM ($N=6$)	3.22321	6.44641	9.66978	12.9774	16.3648	24.5063	30.4161
Galerkin projection ($N=7$)	3.22321	6.44641	9.66962	12.8928	16.1160	19.3392	22.5624

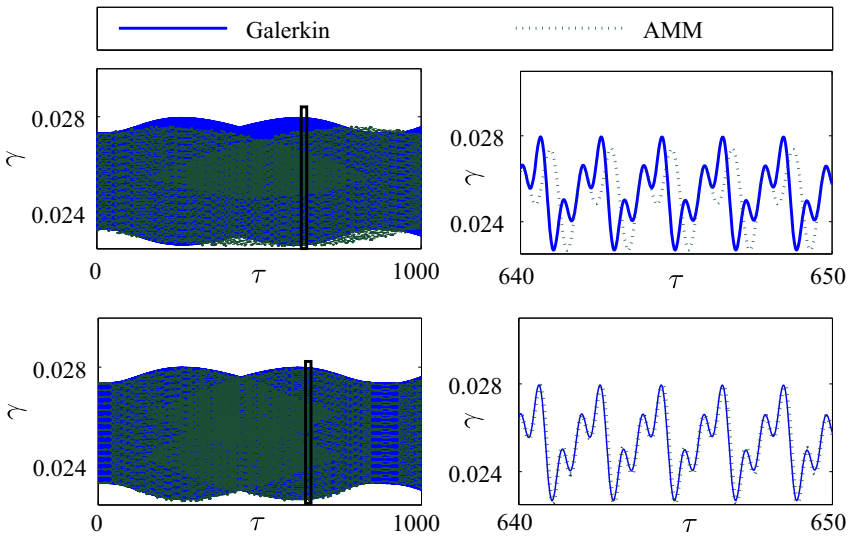

Fig. 12. Left top: comparison of wrapped length (γ) for two different approaches. For Galerkin projection method (blue), $N=3$ and initial conditions are zero except $\beta_1(0)=2$. For AMM (green), $N=3$ and initial conditions are $\gamma(0)=0.0233081394, \beta_1(0)=-3.821692978, \beta_2(0)=7.327507837, \beta_3(0)=1.036301708$. Other parameter values are $b=0.05, \alpha=4/b^2$ and $h_r=0$. Right top: a magnified view of the boxed portion from the left. Left bottom: same as top except for the AMM for which $N=6$ and the initial conditions are $\gamma(0)=0.0233081394, \beta_1(0)=-3.814181522, \beta_2(0)=7.312481007, \beta_3(0)=1.541336782, \beta_4(0)=-2.719259225, \beta_5(0)=-0.3191401979, \beta_6(0)=0.5266884477$. Right bottom: a magnified view of the boxed portion from the left bottom. (For interpretation of the references to color in this figure caption, the reader is referred to the web version of this paper.)

(the Galerkin projection technique) and (69) (the AMM) are tabulated in Table 1 for the parameter values $b=0.05$ and $\alpha=4/b^2$. Natural frequencies from the alternate method are clearly approaching the natural frequencies obtained from (46) with an increase in the number of terms N thereby increasing our confidence in the results obtained earlier.

5.2. Nonlinear analysis

To further verify our observations about the solutions, we have numerically simulated the system of equations given by (67) and (68) simultaneously using the Matlab ode45 solver for the same initial string configuration and the same parameter values which are used to solve (62). Since the modal coordinates for these two different approaches are different from each other, hence we cannot compare them directly. However, we can compare the evolution of the global quantities like the wrapped length (γ) of the string over the bridge with time. Fig. 12 shows the wrapped length for the two different approaches for a different number of terms in the two approximations. From the top plots in Fig. 12 we can observe that the solutions obtained from the two different approaches for the wrapped length for the same size of the approximation ($N=3$) for both are not exactly the same but they show some qualitative similarities. However, from the bottom plots in Fig. 12 we can see that with a higher value of $N=6$ for the AMM, the results obtained from the two different approaches are quantitatively similar as well. This is because of a slower convergence rate for the AMM. However, the quantitative agreement between the results from the two approaches reinforces our confidence on the correctness of the solutions reported in this paper. We have also checked the match between the other global quantities viz. the kinetic and potential energies, and they show the same trend as γ. These plots have not been reported here for brevity.

6. Conclusion

We have derived the governing equation of motion and the boundary conditions for a string vibrating against a smooth unilateral obstacle at one of the ends akin to the situation in several musical instruments used in Indian classical music like the sitar and the veena. The problem of a moving boundary due to the wrapping and unwrapping of the string over the obstacle has been converted into a fixed boundary problem by a dynamic scaling of the spatial variable. This scaling introduces nonlinearity into the governing equation of motion. We have investigated the free vibration characteristics viz. the natural frequencies and mode-shapes of the system by linearizing the obtained governing equations of motion and found that the natural frequencies are harmonic. Hence, the model presented in this study does not explain the better harmonic nature of the sound of the instruments like sitar and veena with a string of finite bending stiffness compared to their western counterparts. Analytical expressions have been obtained for the time-varying mode shapes as well as the nodal points associated with these modes. These variations can potentially lead to frequency modulations as well as appearance of higher overtones which are a prominent feature of the musical instruments under consideration. A numerical study of the fully nonlinear model shows modal interactions between different modes which explain the amplitude modulations reported for these musical instruments. We have verified our results by obtaining all the results from two different alternate approaches with different representations for the string displacements and the results from both the approaches show a very good agreement with each other. Our analysis shows that amplitude and frequency modulations for different modes as well as appearance of higher overtones which are distinguishing characteristic features of musical instruments like sitar and veena are primarily due to the presence of a finite sized bridge over which the string wraps and unwraps smoothly without impacts. The better harmonic nature of the sound of these musical instruments is not explained by our current model and a coupled structure–string vibration model accounting for the motion of the bridge might be required to explain this phenomenon which will be carried out in our future study.

Appendix A. Natural frequencies with a more realistic bridge shape

In this paper, our results and discussion were based on the assumption that the shape of the bridge is parabolic with maximum height at the middle of the length of the bridge. However, our concern is a type of musical instrument where height of the bridge is maximum near the string termination end. Fig. A1 shows a more realistic model where the bridge shape is different from the previous model. Here we characterize the bridge with three parameters, the left hand height of the bridge H_1, right hand height of the bridge H_2, and slope M_1 of the bridge at the left end. The geometry of the bridge can be written as

$$Y_B = \left[\frac{H_2 - H_1}{B^2} - \frac{M_1}{B}\right] X^2 + M_1 X + H_1 \tag{70}$$

whose non-dimensional form is

$$y_b = a_1 x^2 + m_1 x + h_1, \tag{71}$$

where $a_1 = (h_2 - h_1)/b^2 - m_1/b$ and the nondimensional quantities are $h_1 = H_1/h, h_2 = H_2/h$, and $m_1 = (L/h)M_1$. This new shape of the bridge (70) does not affect the equation of motion (30). Choosing solutions of the form (33) and (34) leads us to the same linearized equation (36). However, this new geometry of the bridge changes the boundary conditions (31) and (32) to

$$y(0,\tau) = a_1\gamma^2 + m_1\gamma + h_1, \quad y(1,\tau) = h_r, \tag{72}$$

$$\left.\frac{\partial y(x,\tau)}{\partial x}\right|_{x=0} = (2a_1\gamma + m_1)(1-\gamma), \tag{73}$$

where we redefined $h_r = H_r/h$. Now, we substitute (33) and (34) into (72) and (73). Separating terms of different orders of ϵ and equating them to zero result in

$$y_{st}(0,\tau) = a_1\gamma_{st}^2 + m_1\gamma_{st} + h_1, \quad \tilde{y}(0,\tau) = (2a_1\gamma_{st} + m_1)\tilde{\gamma}(\tau), \quad y_{st}(1,\tau) = h_r, \quad \tilde{y}(1,\tau) = 0, \tag{74}$$

$$a_1\gamma_{st}^2 - 2a_1\gamma_{st} - (m_1 + h_1 - h_r) = 0, \quad \left.\frac{\partial\tilde{y}}{\partial x}\right|_{x=0} = 2a_1 - 4a_1\gamma_{st} - m_1. \tag{75}$$

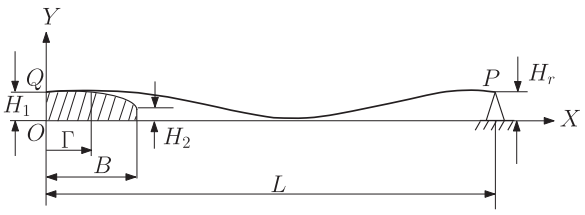

Fig. A1. String model with a more realistic bridge shape.

Conveniently, for $\tilde{y}(x,\tau)$ we choose

$$\tilde{y}(x,\tau) = (2a_1\gamma_{st} + m_1)\tilde{\gamma}(1-x) + \sum_{i=0}^{N} \beta_i(t)\ \sin(i\pi x). \tag{76}$$

Following the Galerkin projection technique, using (75) and (76), the reduced order model of (36) is

$$\ddot{\beta}_m(t) + \frac{m^2\pi^2}{(1-\gamma_{st})^2}\beta_m(t) = 0. \tag{77}$$

Therefore, the natural frequencies for this case are the same as that of the case discussed in Section 3. The only effect of the changed geometry is to modify the length of the wrapped portion of the string in the static configuration γ_{st} and accordingly, modify the individual frequencies. However, the fact that the various natural frequencies are harmonic of the fundamental frequency for our model remains the same.

References

[1] B.C. Deva, *Musical Instruments of India: Their History and Development*, 2nd ed. Munshiram Manoharlal, New Delhi, India, 1987.
[2] C.V. Raman, On some Indian stringed instruments, *Proceedings of the Indian Association for the Cultivation of Science* 7 (1921) 29–33.
[3] V.L. Janakiram, B. Yegnarayana, Temporal variation of tonal spectrum of tambura, *The 94th Meeting of the Acoustical Society of America*, Miami Beach, Florida, 1977 (Abstract available at the *Journal of the Acoustical Society of America*, 62(S1), S43).
[4] A.J.M. Houtsma, E.M. Burns, Temporal and spectral characteristic of tambura tones, *The 103rd Meeting of the Acoustical Society of America*, Chicago, Illinois, 1982 (Abstract available at the *Journal of the Acoustical Society of America*, 71(S1), S83).
[5] A.H. Benade, W.G. Messenger, Sitar spectrum properties, *The 103rd Meeting of the Acoustical Society of America*, Chicago, Illinois, 1982 (Abstract available at the *Journal of the Acoustical Society of America*, 71(S1), S83).
[6] R. Sengupta, B.M. Banerjee, S. Sengupta, D. Nag, Tonal quality of the Indian tanpura, *Proceeding of International Symposium—Stockholm Music Acoustics Conference (SMAC)*, Speech Transmission Laboratory, Royal Institute of Technology, Sweden, 1983.
[7] S. Le Conte, S. Vaiedelich, P. Bruguiere, Acoustical measurement of Indian musical instruments (Vinas): towards greater understanding for better conservation, Acoustics Paris'08, 2008 (Abstract available at the *Journal of the Acoustical Society of America*, 123(5), 3380).
[8] P.G. Singh, Perception and orchestration of melody, harmony and rhythm on instruments with 'chikari' strings, *Proceedings of Meetings on Acoustics—ICA 2013*, Montreal, Canada, 2013 (Abstract available at the *Journal of the Acoustical Society of America*, 133(5), 3448).
[9] C.R. Bahn, Extending and abstracting sitar acoustics in performance, *Noise-Con 2010*, Baltimore, Maryland, 2010 (Abstract available at the *Journal of the Acoustical Society of America*, 127(3), 2011).
[10] S. Weisser, M. Demoucron, Shaping the resonance. Sympathetic strings in Hindustani classical instruments, *Acoustics 2012 Hong Kong*, 2012 (Abstract available at the *Journal of the Acoustical Society of America*, 131(4), 3330).
[11] E.V. Carterette, N. Jairazbhoy, K. Vaughn, The role of tambura spectra in drone tunings of North Indian ragas, *The 115th Meeting of the Acoustical Society of America*, Seattle, Washington, 1988 (Abstract available at the *Journal of the Acoustical Society of America*, 83(S1), S121).
[12] C. Valette, C. Cuesta, M. Castellengo, C. Besnainou, The tampura bridge as a precursive wave generator, *Acoustica* 74 (1991) 201–208.
[13] T. Taguti, Y. Tohnai, Acoustical analysis on the sawari tone of Chikuzen biwa, *Acoustical Science and Technology* 22 (3) (2001) 199–208.
[14] L. Amerio, Continuous solution of the problem of a string vibrating against an obstacle, *Rendiconti del Seminario Matematico della Universit di Padova* 59 (1978) 67–96.
[15] M. Schatzman, A hyperbolic problem of second order with unilateral constraints: *the vibrating string with a concave obstacle*, *Journal of Mathematical Analysis and Application* 73 (1980) 138–191.
[16] R. Burridge, J. Kappraff, C. Morshedi, The sitar string, a vibrating string with a one sided inelastic constant, *SIAM Journal of Applied Mathematics* 42 (6) (1982) 1231–1251.
[17] J. Ahn, A vibrating string with dynamic frictionless impact, *Applied Numerical Mathematics* 57 (2007) 861–884.
[18] T. Taguti, Dynamics of simple string subject to unilateral constraint: *a model analysis of sawari mechanism*, *Acoustical Science and Technology* 29 (3) (2008) 203–214.
[19] C.P. Vyasarayani, S. Birkett, J. McPhee, Modeling the dynamics of a vibrating string with finite distributed unilateral constraint: *application to the sitar*, *Journal of the Acoustical Society of America* 125 (6) (2009) 3673–3682.
[20] A. Alsahlani, R. Mukherjee, Vibration of a string wrapping and unwrapping around an obstacle, *Journal of Sound and Vibration* 329 (2010) 2707–2715.
[21] G.S.S. Murthy, B.S. Ramakrishna, Nonlinear character of resonance in stretched strings, *Journal of the Acoustical Society of America* 38 (3) (1965) 461–471.
[22] J. Elliott, Intrinsic nonlinear effects in vibrating strings, *American Journal of Physics* 48 (6) (1980) 478–480.
[23] C.P. Vyasarayani, S. Birkett, J. McPhee, A vibrating sitar string: modeling the 3D dynamics of a plucked string impacting a special obstacle with friction, *Acoustics Paris'08*, 2008 (Abstract available at the *Journal of the Acoustical Society of America*, 123(5), 3380).
[24] G. Suweken, W.T. van Horssen, On the transversal vibrations of a conveyor belt with a low and time-varying velocity. Part I: *the string-like case*, *Journal of Sound and Vibration* 264 (2003) 117–133.
[25] S.H. Sandilo, W.T. van Horssen, On variable length induced vibrations of a vertical string, *Journal of Sound and Vibration* 333 (2014) 2432–2449.
[26] A. Roy, A. Chatterjee, Vibrations of a beam in variable contact with flat surface, *Journal of Vibration and Acoustics* 131 (4) (2009) 0410101–0410107.
[27] I.M. Gelfand, S.V. Fomin, in: R.A. Silverman (Ed.), *Calculus of Variations*, Dover Publications, INC. Mineola, New York, 2000, pp. 59–61.